SCIENTIFIC REPORTS

OPEN

SUBJECT AREAS:
INORGANIC CHEMISTRY
MATERIALS CHEMISTRY
SUPRAMOLECULAR CHEMISTRY
CHEMISTRY

Received
30 May 2012

Accepted
22 August 2012

Published
18 September 2012

Correspondence and requests for materials should be addressed to T.-B.L. (lutongbu@mail.sysu.edu.cn)

Constructions of two polycatenanes and one polypseudo-rotaxane by discrete tetrahedral cages and stool-like building units

Long Jiang, Ping Ju, Xian-Rui Meng, Xiao-Jun Kuang & Tong-Bu Lu

MOE Key Laboratory of Bioinorganic and Synthetic Chemistry, State Key Laboratory of Optoelectronic Materials and Technologies, and School of Chemistry and Chemical Engineering, Sun Yat-Sen University, Guangzhou 510275, China.

Mechanically Interlocked molecules, such as catenanes and rotaxanes, are of great interest due to their fascinating structures and potential applications, while such molecules have been mainly restricted to comprising components of interlocked rings or polygons. The constructions of infinite polycatenanes and polyrotaxanes by discrete cages remain great challenge, and only two infinite polycatenanes fabricated by discrete cages have been reported so far, while the structures of polyrotaxanes and poly*pseudo*-rotaxanes fabricated by discrete build units have not been documented to date. Herein we report the first example of a two-dimensional (2D) poly*pseudo*-rotaxane fabricated by stool-like build units, the second example of a one-dimensional (1D) polycatenane, and the second example of a three-dimensional (3D) polycatenane, which were assemblied by discrete tetrahedral cages. The pores of dehydrated 3D polycatenane are dynamic, and display size-dependent adsorption/desorption behaviors of alcohols.

The design and synthesis of interlocked molecules such as catenanes and rotaxanes, in which components are held together by mechanical linkages rather than by chemical covalent bonds, have attracted extensive interests, not only for their remarkable structural prototypes of molecular machines[1–5], molecular motors[6–8], and molecular knots[9], but also for their potential applications in information processing and storage[10], molecular electronics[11], light-driven molecular machines[12], and catalysis[13]. An efficient strategy for the constructions of catenanes and rotaxanes is to use discrete coordination cages as components to construct interlocked structures[14], while such examples are still limited. In 1999, Fujita and co-workers firstly reported a structure of [2]catenane, which was assemblied from two discrete interlocked coordination cages[15]. Ten years later, the second and third structures of [2]catenanes by two discrete coordination cages have been reported by Hardie[16] and Kuroda et al[17], respectively, and the fourth [2]catenane displaying the same interlocked motif as that of the second [2]catenane has been reported by Hardie and coworkers in 2011[18]. However, all the above four reported [2]catenanes are confined to duple intercatenation of discrete cages, the constructions of infinite polycatenanes fabricated by mechanical interlocking of discrete polyhedral cages remain more challenging.

Despite the fact that both infinite metal-organic frameworks including polycatenanes and polyrotaxanes have been extensively investigated for over two decades, to the best of our knowledge, only two infinite polycatenanes fabricated by mechanical interlocking of discrete cages have been reported so far. One of such example is a three-dimensional (3D) infinite polycatenated framework constructed from adamantane-like coordination cages reported by Lu and coworkers[19], the other example is a one-dimensional (1D) strandlike polycatenane constructed from icosahedral cages by Dehnen and coworkers[20]. The structures of polyrotaxanes and poly*pseudo*-rotaxanes fabricated by discrete build units have not been documented to date. Herein, we report the second example of a 1D polycatenane of $\{[NiL]_4(Htcba)_4(H_2O)_2\}$ (**1**), the first example of a two-dimensional (2D) poly*pseudo*-rotaxane of $\{[NiL]_5(tcba)_3(PF_6)(H_2O)_2\}$ (**2**), and the second example of a 3D polycatenane of $\{H[NiL]_6(tcba)_4(ClO_4)\}$ (**3**), which are constructed from discrete tetrahedral cages and stool-like build units. (L = 1,4,8,11-tetraazaundecane, H_3tcba = tri(4-carboxy- benzyl)amine, see Fig. 1).

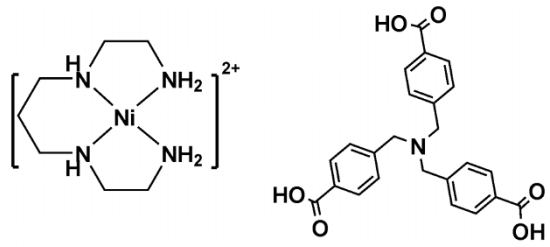

Figure 1 | The structures of $[NiL]^{2+}$ (left) and H_3tcba (right).

Results

Layering an aqueous solution of H_3tcba with a DMF solution of $[NiL]Cl_2$ generated needle-shaped pink crystals of **1**·$35H_2O$. While the evaporation of the mixture solution of MeOH and MeCN (1:1 v/v) containing H_3tcba and $[NiL](PF_6)_2$/$[NiL](ClO_4)_2$ gave the prism-shaped purple crystals of **2**·$43H_2O$ and block-shaped octahedral purple crystals of **3**·$31H_2O$, respectively. The structures of **1** and **2** were solved by single crystal X-ray diffraction, while the structure of **3** could not be refined using the single crystal X-ray diffraction due to the weak diffraction data, the final structure was refined by the Rietveld method using the X-ray powder diffraction data and the initial solution obtained from the single-crystal X-ray diffraction (Supplementary Fig. S1). The compositions of 1–3 were determined by the combined results of X-ray crystal structures, electron probe micro-analyzer (EPMA) measurements (Supplementary Fig. S2), element analyses, and thermogravimetric analyses (Supplementary Fig. S3).

The asymmetric unit of **1** is composed of one $[NiL]^{2+}$ cation and one $Htcba^{2-}$ anion. As shown in Fig. 2a, each Ni(II) ion is six-coordinated to four N atoms from L and two carboxylate O atoms from two individual $Htcba^{2-}$ anions, forming a slightly distorted N_4O_2 octahedral geometry. Each $Htcba^{2-}$ combines two $[NiL]^{2+}$ units through its two 4-carboxy-benzyl groups. In **1**, four $Htcba^{2-}$ anions combine four $[NiL]^{2+}$ cations to form a folded ring of $\{[NiL](Htcba)\}_4$, and four uncoordinated 4-carboxy-benzyl groups are connected by two O1w molecules through the intermolecular hydrogen bonds to generate a closed neutral tetrahedronal cage, in which four $Htcba^{2-}$ locate at four vertexes of the tetrahedral cage, and four Ni(II) and two water molecules locate at the six edges of the tetrahedral cage.

The distances of six tetrahedronal edges are 17.40 ~ 18.02 Å measured by the N···N distances of $Htcba^{2-}$. It is interesting to note that each tetrahedral cage is interlocked with two adjacent tetrahedral cages, generating a 1D infinite polycatenane fabricated by mechanical interlocking of tetrahedral cages along the *c* axis (Fig. 2b), with a distance of 8.88 Å between the centers of two adjacent cages. All the 1D infinite polycatenanes are packed along the *c* axis to generate the structure of **1**, in which each 1D polycatenane is surrounded by four adjacent 1D polycatenanes (Supplementary Fig. S4), with the closest center···center distance of 21.24 Å between two adjacent 1D polycatenanes. To the best of our knowledge, **1** represents the second example of 1D polycatenane, and the first example of 1D polycatenane assemblied from discrete interlocked tetrahedral cages.

The structure of **2** contains a $\{[NiL]_5(tcba)_3(H_2O)_2\}^+$ cation and a PF_6^- anion (Fig. 3a), in which three of five Ni(II) are six-coordinated to four N atoms from L and two carboxylate O atoms from two individual $tcba^{3-}$ anions, and two of five Ni(II) are six-coordinated to four N atoms from L, one carboxylate O atom from $tcba^{3-}$, and one water molecule. In **2**, three $tcba^{3-}$ anions combine five $[NiL]^{2+}$ cations to form a three leg stool-like build unit (Fig. 3a). The three legs of the 'stool' are unsymmetrical, in which two legs contain the $[NiL(H_2O)]^{2+}$ units, while the third leg contains an uncoordinated 4-carboxy-benzyl group only. Each stool-like build unit contains a PF_6^- anion. The most striking feature of **2** is that each 'stool' is threaded to three adjacent 'stools' through its three legs (Fig. 3b) to generate a novel 2D poly*pseudo*-rotaxane (Fig. 3c), in which two

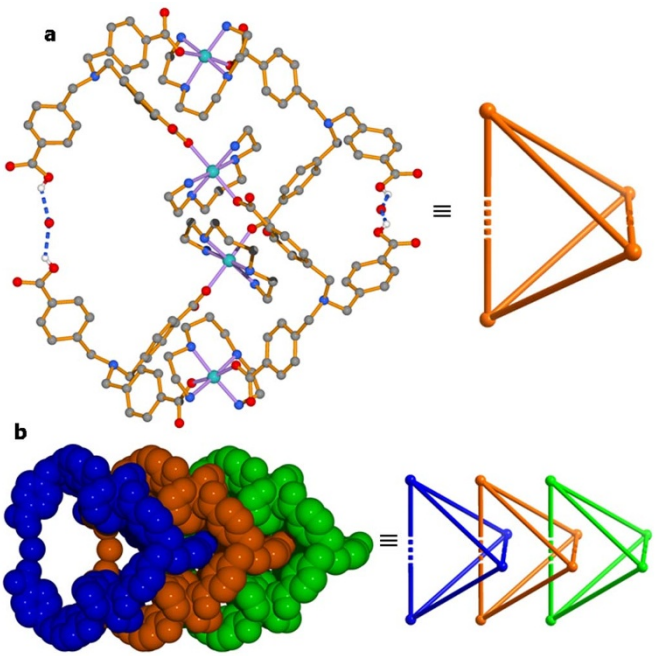

Figure 2 | The structure of 1. (a) The structure of a discrete tetrahedral cage. (b) Space-filling and ball-and-stick representations of a 1D polycatenane assemblied from discrete interlocked tetrahedral cages (L and H atoms are omitted for clarity, the different colors represent three different interlocked cages).

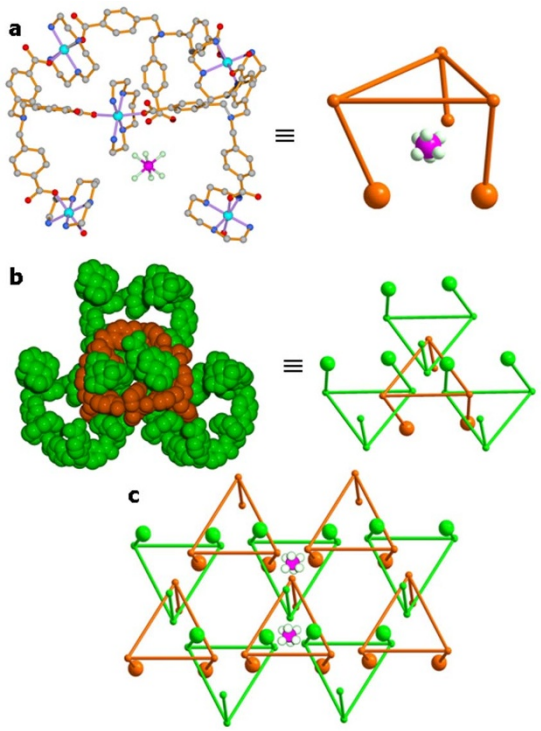

Figure 3 | The structure of 2. (a) A three leg stool-like structure of $\{[NiL]_5(tcba)_3(H_2O)_2\}(PF_6)$. (b) and (c) Space-filling and ball-and-stick representations of 2D poly*pseudo*-rotaxane (the large and small balls at the end of the legs represent the $[NiL(H_2O)]^{2+}$ unit and uncoordinated 4-carboxy-benzyl group, respectively).

coordinated $[NiL(H_2O)]^{2+}$ units act as stopper. To the best of our knowledge, such 2D poly*pseudo*-rotaxane structure has not been reported so far.

In **3**, four $tcba^{3-}$ anions connect six $[NiL]^{2+}$ cations through its three 4-carboxy-benzyl groups to form a tetrahedral cage of $[NiL]_6(tcba)_4$ (Fig. 4a), in which each Ni(II) is six-coordinated to four N atoms from L and two carboxylate O atoms from two individual $tcba^{3-}$ anions, and each $tcba^{3-}$ connects three $[NiL]^{2+}$. Four $tcba^{3-}$ locate at four vertexes of the tetrahedral cage, and six Ni(II) locate at the six edges of the tetrahedral cage. The distances of six edges of the tetrahedral cage, 16.64 Å (measured by the N···N distances of $tcba^{3-}$), are shorter than those of 17.40 ~ 18.02 Å in **1**. Each cage contains a ClO_4^- and a proton, while the position of the proton can not be located. It is likely that the ligand L/tbca is single protonated, or one of the waters of crystallization elsewhere in the crystal lattice has been protonated.

Up to now, a numbers of tetrahedral cages with a composition of M_4L_6 have been reported[21], in which the metal ions locate at four vertexes of the tetrahedral cage, and six ligands locate at the six edges of the tetrahedral cage. In contrast, the tetrahedral cage we present here has a composition of M_6L_4 rather than M_4L_6.

The most aesthetically pleasing structural feature of **3** is its novel polycatenation between discrete tetrahedral cages, in which each cage is interlocked with four adjacent tetrahedral cages through all its four vertices (Fig. 4b, Supplementary Fig. S5), and the overall architecture is produced by mechanical linkages rather than by coordination bonds. The propagation of the quadruple intercatenation of each discrete cage generates an unprecedented 3D extended polycatenated structure of **3**. To our knowledge, **3** represents the second example of 3D polycatenane constructed from discrete cages, and the first example of 3D polycatenane composed of discrete tetrahedral cages. The structure of **3** is different from the previously reported 3D infinite polycatenated structure of $\{[Ag_2(trz)_2][Ag_{24}(trz)_{18}]\}[PW_{12}O_{40}]_2$ (trz = 1, 2, 4,-triazole), which was constructed from adamantane-like coordination cages containing large $[PW_{12}O_{40}]^{3-}$ anions, and the $[PW_{12}O_{40}]^{3-}$ anions reside in the cavities of the adamantane-like cages to generate a nonporous 3D structure. In contrast, the structure of **3** is constructed from tetrahedral cages with a ClO_4^- anion resided in the center of each tetrahedral cage. There are still numbers of void in the structure of **3**, which are filled with guest water molecules due to the small void of ClO_4^- anion, and a solvent accessible volume is 10.1% calculated by PLATON[22].

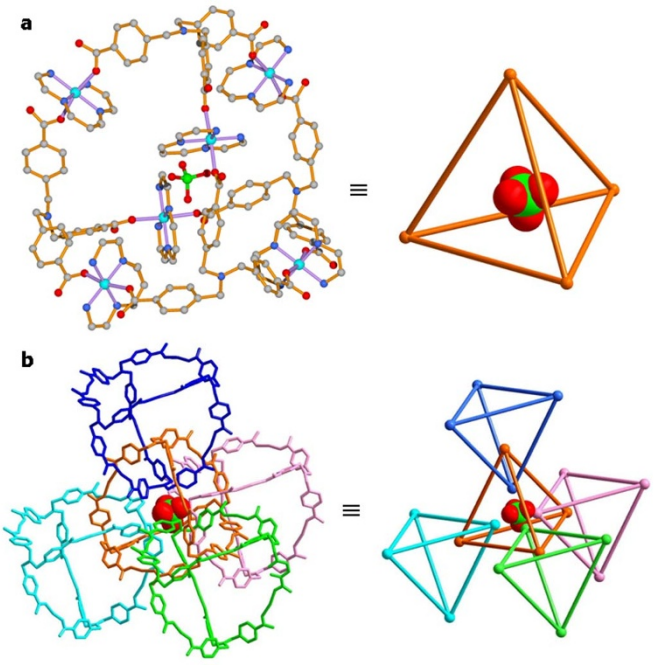

Figure 4 | The structure of 3. (a) The structure of a discrete M_6L_4 tetrahedral cage. (b) The ball-and-stick representation of 3D polycatenane assemblied from discrete interlocked tetrahedral cages (The five interlocked cages are shown with different colors).

The thermogravimetric analysis (TGA) curves of **1** and **2** show a weight loss of 19.3 and 24.2% respectively below 120 °C (Supplementary Fig. S3), corresponding to the removal of thirty seven water molecules for **1** (calcd 20.7%) and forty five water molecules for **2** (calcd 24.5%). The result of TGA indicates the lattice water molecules in **3** can be removed under 130°C (Supplementary Fig. S3), with a weight loss of 15.1% being consistent with the remove of thirty one water molecules (calcd 15.1%). After removal water molecules, the compounds **1**–**3** can be stable around 300°C and then began to decompose upon further heating. The result of X-ray powder diffraction (XRD) measurements of **1**–**3** indicate that all the peaks displayed in the measured pattern closely matches those in the simulated pattern generated from single-crystal diffraction data (Supplementary Fig. S6), indicating a single phase of **1**–**3** was formed. The variable temperature XRD measurements for **3** indicate that the framework of **3** can be stable up to 130°C. The results of N_2 (77 K), H_2 (77 K) and CO_2 (195 K) adsorption measurements indicate that the dehydrated **3** becomes nonporous after removal of guest water molecules (Supplementary Fig. S7).

To check the adsorption properties of **3** and to examine if the framework of **3** can be reversibly formed upon dehydration and hydration, a crystalline sample of **3** was dried at 100°C for 20 min, and the XRD pattern is different from that of the as-isolated sample (Supplementary Fig. S6), indicating a structural change upon guest water removal. However, when the dried sample was exposed to air for 2 h, the XRD pattern is almost the same as that of the as-isolated, indicating the recovery of the original framework after guest molecule adsorption, and the framework of **3** is dynamic, the results of TGA measurements also demonstrate that dehydrated **3** absorbed water molecules reversibly from the air (Supplementary Fig. S8). In order to further understand the sorption properties of dynamic framework of **3**, a series of alcohols sorption measurements were carried out in a relative pressure range from 0.01 to 0.92 atm. The results indicate that the dehydrated **3** can adsorb methanol, ethanol, *iso*-propanol and *tert*-butyl alcohol (Fig. 5). Interestingly, the sorption isotherms of methanol, ethanol and *iso*-propanol at 299 K, and *tert*-butyl alcohol at 305 K show obvious hysteresis loops, and the hysteresis loops become larger along with the increase sizes from methanol to *tert*-butyl alcohol, indicating the adsorbed alcohols become more difficult to desorb along with the increasing sizes of alcohols[23]. In addition, the numbers of adsorbed alcohols per tetrahedral cage decrease along with the increase sizes of alcohols (Fig. 5) The sizes dependent adsorption/desorption behaviors of dehydrated **3** is attributed to the dynamic pores generated by the interlocked cages. The results of XRD measurements indicate that the position of the peak at 18.55° for dehydrated **3** moved to lower degree after the adsorption of alcohols (Supplementary Fig. S9), and the unit cell parameters and volume for dehydrated **3** increase from 33.08(1) Å and 36195(47) $Å^3$ to 33.467(4)~33.65(2) Å and 37486(14)~38093(55) $Å^3$ after the adsorption of alcohols (Supplementary Table S4), further demonstrating the pores in dehydrated **3** are dynamic. It's interesting to note that the unit cell parameters and volumes decrease along with the increase sizes of alcohols (Supplementary Table S4), consisting with the result that the numbers of adsorbed alcohols per tetrahedral cage decrease along with the increase sizes of alcohols. Such a guest molecular size-dependent structural responsiveness is rarely observed in the common porous materials, and provides a unique entry into the development of functional materials for guest separation and sensor.

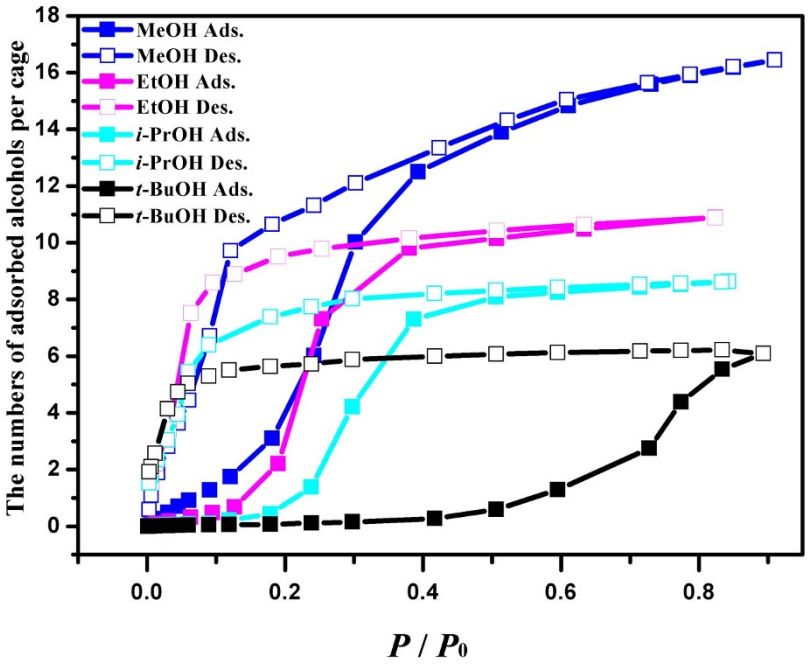

Figure 5 | Sorption properties. Sorption isotherms of MeOH, EtOH, *i*-PrOH and *t*-BuOH vapor for dehydrated **3**.

Discussion

In summary, a 1D polycatenane of **1** and a 3D polycatenane of **3** were successfully constructed by the intercatenation of discrete tetrahedral cages, and a 2D poly*pseudo*-rotaxane of **2** assemblied from three leg stool-like build units was firstly obtained. In addition, the framework of **3** is dynamic, and dehydrated **3** displays guest molecular size-dependent adsorption/desorption behaviors of alcohols, which can be potentially used as functional materials for guest separation and sensor.

Methods

Materials. All materials were purchased from commercially available sources and used without further purification. $[NiL]Cl_2$ was synthesized by the literature method[24]. $[NiL](PF_6)_2$ and $[NiL](ClO_4)_2$ were prepared from $[NiL]Cl_2$ through changing chloride with hexafluorophosphate and perchlorate, respectively. H_3tcba was prepared according to the previously reported method[25].

Measurements. Elemental analyses were determined using Elementar Vario EL elemental analyzer. The IR spectra were recorded in the 4000∼400 cm^{-1} region using KBr pellets and a Bruker EQUINOX 55 spectrometer. TG analyses were performed on a Netzsch TG 209 instrument under nitrogen atmosphere with a heating rate of 10°C/min. Variable-temperature X-ray powder diffraction measurements were performed on a Bruker D8 ADVANCE X-ray diffractometer. EPMA measurements were performed on a JXA-8800R electron probe micro-analyzer. MeOH, EtOH, *i*-PrOH and *t*-BuOH vapor adsorption-desorption isotherm measurements were carried out using an Hiden Intelligent Gravimetric Analyzer (IGA-003). The initial outgassing process for the sample was carried out under a high vacuum (less than 10^{-6} mbar) at 100°C for 5 h. The degassed sample and sample tube were weighed precisely and transferred to the analyzer. MeOH, EtOH and *i*-PrOH vapor adsorption/desorption were measured at 299 K, while *t*-BuOH was measured at 305 K.

Caution! Perchlorate salts of metal complexes with organic ligands are potentially explosive. They should be handled with care, and prepared only in small quantities.

$\{[NiL]_4(Htcba)_4(H_2O)_2\}$ (**1**). An aqueous solution (4 mL) of H_3tcba (34 mg, 0.08 mmol) and NaOH (10 mg, 0.24 mmol) was layered with a DMF solution (6 mL) of $[NiL]Cl_2$ (34 mg, 0.12 mmol) at room temperature. After about two months, needle-shaped pink crystals suitable for X-ray analysis formed. Yield: 6 mg, 6% based on $[NiL]Cl_2$. EA calculated (%) for $C_{124}H_{226}N_{20}O_{59}Ni_4$ (**1**·$33H_2O$): C 46.89, H 7.17, N 8.82; found: C 46.79, H 7.49, N 8.82. IR (KBr): ν = 3355 (w), 3274 (w), 2950 (w), 2929 (w), 2868 (w), 1933 (w), 1816 (w), 1595 (vs), 1552 (vs), 1464 (w), 1387 (vs), 1293 (w), 1244 (m), 1171 (w), 1104 (w), 1018 (w), 975 (m), 812 (m), 776 (m), 709 (w), 661 (w), 635 (w), 528 (w), 449 (w) cm^{-1}.

$\{[NiL]_5(tcba)_3(H_2O)_2(PF_6)\}$ (**2**). A mixture solution of methanol and acetonitrile (30 mL, 1:1 v/v) containing H_3tcba (34 mg, 0.08 mmol) and $[NiL](PF_6)_2$ (44 mg, 0.12 mmol) was evaporated slowly at room temperature to get prism-shaped purple crystals of **2**·$43H_2O$. Yield: 16 mg, 20% based on $[NiL](PF_6)_2$. EA calculated (%) for $C_{107}H_{244}N_{23}O_{63}F_6PNi_5$ (**2**·$43H_2O$): C 38.94, H 7.45, N 9.76; found: C 38.90, H 7.68, N 9.79. IR (KBr): ν = 3358 (w), 3274 (w), 2951 (w), 2931 (w), 2871 (w), 1664 (vs), 1595 (vs), 1552 (vs), 1462 (w), 1388 (vs), 1290 (w), 1246 (m), 1171 (w), 1103 (w), 1057 (w), 1018 (w), 976 (m), 846 (s), 777 (m), 736 (w), 710 (w), 662 (w), 634 (w), 559 (m), 528 (w), 450 (w) cm^{-1}.

$\{H[NiL]_6(tcba)_4(ClO_4)\}$ (**3**). Octahedron-shaped purple crystals of **3**·$31H_2O$ were obtained by a similar procedure to that of **2**, except using $[NiL](ClO_4)_2$ instead of $[NiL](PF_6)_2$. Yield: 35 mg, 48% based on $[NiL](ClO_4)_2$. EA calculated (%) for $C_{138}H_{255}N_{28}O_{59}ClNi_6$ (**3**·$31H_2O$): C 45.56, H 7.01, N 10.78; found: C 45.53, H 7.36, N 10.80. IR (KBr): ν = 3355 (m), 3273 (m), 2929 (m), 2869 (m), 1595 (vs), 1551 (vs), 1462 (m), 1387 (vs), 1287 (w), 1172 (w), 1105 (m), 1057 (w), 1018 (s), 975 (s), 886 (w), 866 (w), 850 (w), 811 (w), 776 (m), 710 (w), 661 (w), 633(w), 528 (w), 450 (w) cm^{-1}.

X-ray single crystal structure analyses. Diffraction data were collected on an Agilent Gemini S Ultra diffractometer with the Enhance X-ray Source of Cu radiation (λ = 1.54178 Å). All empirical absorption corrections were applied using spherical harmonics implemented in SCALE3 ABSPACK scaling algorithm[26]. The structures were solved using direct methods, which yielded the positions of all non-hydrogen atoms. The atomic displacement factors were refined first isotropically and then anisotropically. All the hydrogen atoms of the ligands were placed in the calculated positions with fixed isotropic thermal parameters and were included in the structure factor calculations in the final stage of full-matrix least-squares refinement. The positional disorder of benzoate groups of $tcba^{3-}$ in **1** and **2** and PF_6^- in **2** was treated with FVAR. All of the disordered parts were restrained using DFIX, DELU, and SIMU instructions to achieve reasonable displacement parameters. The hydrogen atoms of all lattice water molecules in **1** and **2** were not added. All calculations were performed using the SHELXTL system of computer programs[27]. For **3**, the structure was solved by direct methods, and the refined methods are similar to those for **1** and **2**. $tcba^{3-}$. $[NiL]^{2+}$ groups exhibit orientational disorder over two sets of positions. The hydrogen atoms were generated theoretically onto the specific atoms and refined isotropically with fixed atomic displacement factors. The water molecules in **3** could not be successfully located from the difference-Fourier map calculation due to the weak diffraction data and the disorder of water molecules in the high symmetrical structure, and the water contents in **3** were deduced by means of EA and TGA. The very weak diffraction of the crystal and the absence of water molecules lead to the high R_1 and wR_2 values. All attempts to obtain a better diffraction data were unsuccessful. The final structure of **3** was determined by the Rietveld method using the X-ray powder diffraction data referring to the initial framework obtained from the single-crystal X-ray diffraction. The crystallographic data are summarized in Supplementary Table S1, the final Rietveld refinement parameters are listed in Supplementary Table S2, and the selected bond lengths and angles are listed in Supplementary Table S3. CCDC numbers are 893141-893143 for **1**–**3**, respectively.

X-ray powder diffraction analysis. X-ray powder diffraction pattern of **3** was obtained on a Bruker D8 ADVANCE with Cu Kα radiation (40 kV, 40 mA). The sample of **3** was ground with an agate pestle to get fine powder, and the X-ray diffraction data were recorded in the range of 5–80° 2θ in step scan mode. The structural model for the Rietveld analysis of **3** was taken from the single crystal refinement as initial atomic positions of the framework. The Rietveld refinement was performed using Topas academic software[28]. Distance and angle restraints were

applied for ClO_4^- tetrahedron, NiO_2N_4 octahedron, and planar benzoate group *etc.* during the refinement of atomic positions. Difference Fourier transformation calculation was not successful to determine the oxygen positions of guest water molecules using both single crystal (100 K) and powder (ambient temperature) diffraction data, which was ascribed to the low signal/background ratio in high 2θ range (Supplementary Fig. S1). The oxygen positions of guest water molecules were initially placed as random positions (192i sites (x, y, z)), which were refined by a simulated annealing approach with minimum contact constraints of 2.7Å with framework oxygen, nitrogen and carbon atoms. The occupancies on the oxygen positions of guest water molecules were refined simultaneously. This approach only generated two oxygen sites of guest water molecules (two 96g sites (x, x, z) Ow1 and Ow2 in CIF) with near half occupation for each site, giving a total numbers of guest water molecules of 96 in the unit cell. The powder X-ray diffraction data is not of sufficient quality to fully determine such disordered oxygen positions of guest water molecules in a solvent accessible volume of 3579.9 $Å^3$ per unit cell without ambiguity here. The refinement converged to $R_{wp} = 2.72\%$, $R_p = 1.85\%$, and $R_B = 0.56\%$.

1. Dietrich-Buchecker, C. O. & Sauvage, J. P. Interlocking of molecular threads: from the statistical approach to the templated synthesis of catenands. *Chem. Rev.* **87**, 795–810 (1987).
2. Amabilino, D. B. & Stoddart, J. F. Interlocked and intertwined structures and superstructures. *Chem. Rev.* **95**, 2725–2828 (1995).
3. Swiegers, G. F. & Malefetse, T. J. New self-assembled structural motifs in coordination chemistry. *Chem. Rev.* **100**, 3483–3537 (2000).
4. Carlucci, L., Ciani, G. & Proserpio, D. M. Polycatenation, polythreading and polyknotting in coordination network chemistry. *Coord. Chem. Rev.* **246**, 247–289 (2003).
5. Jin, C. M., Lu, H., Wu, L. Y. & Huang, J. A new infinite inorganic [*n*]catenane from silver and bis(2-methylimidazolyl)methane ligand. *Chem. Commun.* 5039–5041 (2006).
6. Sauvage, J. P. Transition metal-containing rotaxanes and catenanes in motion: toward molecular machines and motors. *Acc. Chem. Res.* **31**, 611–619 (1998).
7. Balzani, V., Credi, A., Raymo, F. M. & Stoddart, J. F. Artificial molecular machines. *Angew. Chem. Int. Ed.* **39**, 3348–3391 (2000).
8. Hernández, J. V., Kay, E. R. & Leigh, D. A. A reversible synthetic rotary molecular motor. *Science* **306**, 1532–1537 (2004).
9. Wang, L., Vysotsky, M. O., Bogdan, A., Bolte, M. & Böhmer, V. Multiple catenanes derived from calix[4]arenes. *Science* **304**, 1312–1314 (2004).
10. Serreli, V., Lee, C.-F., Kay, E. R. & Leigh, D. A. A molecular information ratchet. *Nature* **445**, 523–527 (2007).
11. Flood, A. H., Stoddart, J. F., Steuerman, D. W. & Heath, J. R. Whence molecular electronics. *Science* **306**, 2055–2056 (2004).
12. Balzani, V., Credi, A. & Venturi, M. Light powered molecular machines. *Chem. Soc. Rev.* **38**, 1542–1550 (2009).
13. Thordarson, P., Bijsterveld, E. J. A., Rowan, A. E. & Nolte, R. J. M. Epoxidation of polybutadiene by a topologically linked catalyst. *Nature* **424**, 915–918 (2003).
14. Beves, J. E., Blight, B. A., Campbell, C. J., Leigh, D. A. & McBurney, R. T. Strategies and tactics for the metal-directed synthesis of rotaxanes, knots, catenanes, and higher order links. *Angew. Chem. Int. Ed.* **50**, 9260–9327 (2011).
15. Fujita, M., Fujita, N., Ogura, K. & Yamaguchi, K. Spontaneous assembly of ten components into two interlocked, identical coordination cages. *Nature* **400**, 52–55 (1999).
16. Westcott, A., Fisher, J., Harding, L. P., Rizkallah, P. & Hardie, M. J. Self-assembly of a 3-D triply interlocked chiral [2]catenane. *J. Am. Chem. Soc.* **130**, 2950–2951 (2008).
17. Fukuda, M., Sekiya, R. & Kuroda, R. A quadruply stranded metallohelicate and its spontaneous dimerization into an interlocked metallohelicate. *Angew. Chem. Int. Ed.* **47**, 706–710 (2008).
18. Henkelis, J. J., Ronson, T. K., Harding, L. P. & Hardie, M. J. M_3L_2 metallocryptophanes: [2]catenane and simple cages. *Chem. Commun.* **47**, 6560–6562 (2011).
19. Kuang, X. *et al*. Assembly of a metal–organic framework by sextuple intercatenation of discrete adamantane-like cages. *Nat. Chem.* **2**, 461–465 (2010).
20. Heine, J., Schmedt auf der Günne, J. & Dehnen, S. Formation of a strandlike polycatenane of icosahedral cages for reversible one-dimensional encapsulation of guests. *J. Am. Chem. Soc.* **133**, 10018–10021 (2011).
21. Ward, M. D. Polynuclear coordination cages. *Chem. Commun.* 4487–4499 (2009).
22. Spek, A. L. PLATON, a multipurpose crystallographic tool, Utrecht University: Utrecht, The Netherlands, (2003).
23. Uemura, K., Yamasaki, Y., Onishi, F., Kita, H. & Ebihara, M. Two-step adsorption on jungle-gym-type porous coordination polymers: dependence on hydrogen-bonding capability of adsorbates, ligand-substituent effect, and temperature. *Inorg. Chem.* **49**, 10133-10143 (2010).
24. Curtis, N. F. & Milestone, N. B. Some compounds of nickel(II) and copper(II) with 1,4,8,11-tetraazaundecane. *Aust. J. Chem.* **27**, 1167–1175 (1974).
25. Jiang, L. *et al.* Variations of structures and gas sorption properties of three coordination polymers induced by fluorine atom positions in azamacrocyclic ligands. *Inorg. Chem.* **51**, 1874–1880 (2012).
26. R. E. D. CrysAlis, Oxford Diffraction Ltd. Version 1.171.31.7 (2006).
27. Sheldrick, G. M. SHELXS 97, program for crystal structure refinement, University of Göttingen: Göttingen, (1997).
28. Coelho, A. A. TOPAS-Academic V4; Coelho Software: Brisbane, Australia, (2005).

Acknowledgments

This work was supported by 973 Program of China (2012CB821705) and NSFC (Grant Nos. 21001119, 21121061, 91127002 and 20831005). L.J. thanks Sun Yat-Sen University Foundation for Young Teachers Development Program.

Author contributions

L.J. and T.B.L. conceived and designed the experiments. L.J., P.J. and X.R.M. conducted synthetic experiments. L.J. performed the crystal-structure analyses. X.J.K. performed X-ray powder diffraction analysis. L.J. and P.J. performed sorption measurements. L.J. analysed the data. L.J. and T.B.L. wrote the manuscript. All authors discussed the results and commented on the manuscript.

Additional information

Supplementary information accompanies this paper at http://www.nature.com/scientificreports

Competing financial interest: The authors declare no competing financial interests.

How to cite this article: Jiang, L., Ju, P., Meng, X., Kuang, X. & Lu, T. Constructions of two polycatenanes and one polypseudo-rotaxane by discrete tetrahedral cages and stool-like building units. *Sci. Rep.* **2**, 668; DOI:10.1038/srep00668 (2012).